LETTER

doi:10.1038/nature12150

Enantiomer-specific detection of chiral molecules via microwave spectroscopy

David Patterson[1], Melanie Schnell[2,3] & John M. Doyle[1]

Chirality plays a fundamental part in the activity of biological molecules and broad classes of chemical reactions, but detecting and quantifying it remains challenging[1]. The spectroscopic methods of choice are usually circular dichroism and vibrational circular dichroism, methods that are forbidden in the electric dipole approximation[2]. The resultant weak effects produce weak signals, and thus require high sample densities. In contrast, nonlinear techniques probing electric-dipole-allowed effects have been used for sensitive chiral analyses of liquid samples[3–7]. Here we extend this class of approaches by carrying out nonlinear resonant phase-sensitive microwave spectroscopy of gas phase samples in the presence of an adiabatically switched non-resonant orthogonal electric field; we use this technique to map the enantiomer-dependent sign of an electric dipole Rabi frequency onto the phase of emitted microwave radiation. We outline theoretically how this results in a sensitive and species-selective method for determining the chirality of cold gas-phase molecules, and implement it experimentally to distinguish between the *S* and *R* enantiomers of 1,2-propanediol and their racemic mixture. This technique produces a large and definitive signature of chirality, and has the potential to determine the chirality of multiple species in a mixture.

Our approach to determining chirality depends only on the parity conserving Hamiltonian of an asymmetric top in an external electric field[8]: the three rotational constants A, B and C and the corresponding dipole moment component magnitudes $|\mu_a|$, $|\mu_b|$ and $|\mu_c|$ determine the rotational energy levels of such a molecule, and further specification of the signs of μ_a, μ_b and μ_c fully determines its chirality (Fig. 1). The sign of any two of the three dipole moment components μ_a, μ_b and μ_c is arbitrary and changes with the choice of axes, whereas the sign of the combined quantity $\mu_a\mu_b\mu_c$ is axis independent and changes sign with enantiomer. Equivalently, any measurement of the combined quantity $\mu_a\mu_b\mu_c$, and indeed any measurement of chirality, is time-even and parity-odd. In the context of direct molecular chirality detection, parity violating energy shifts arising from the weak interaction have been predicted[9–12] and could in principle distinguish enantiomers; but the resultant very small frequency shifts have never been observed and are not relevant to the techniques demonstrated here.

The Rabi frequency describing an electric dipole transition between rotational states of a chiral molecule differs in sign for opposite enantiomers[13], and we demonstrate here theoretically and experimentally that it can be mapped onto the phase of emitted radiation by applying an electric field that varies during the molecular coherence time. This switched electric field, E_x, combined with an applied microwave field, E_z, induces $\hat{y}$-polarized oscillations of the molecules' dipole, causing them to emit radiation polarized along the y axis, orthogonal to both E_x and E_z (Fig. 2). This radiation is detected and amplified, with the extracted signal phase ϕ differing by 180° between left- and right-handed (*S* and *R*) enantiomers and indicating the dominant enantiomer (that is, the sign of the enantiomeric excess), while the signal magnitude V indicates the magnitude of the enantiomeric excess. With known molecular constants A, B, C, μ_a, μ_b and μ_c, the enantiomer-dependent signal can be accurately predicted via numerical integration of the well-known asymmetric-top Hamiltonian (Fig. 2b).

We validate our technique using *R*-, *S*- and racemic 1,2-propanediol. This molecule was chosen because the relevant molecular constants are well characterized (A = 8,572.05 MHz, B = 3,640.10 MHz, C = 2,790.96 MHz, μ_a = 1.2 D, μ_b = 1.9 D, μ_c = 0.36 D; ref. 14) and because it is readily available commercially in enantiopure form. 1,2-propanediol and larger molecules occupy a large number of quantum states at room temperature, which dilutes the signal obtained from a single rotational level (for example, more than 5,000 occupied states for 1,2-propanediol). To reduce the number of occupied states and increase the resonant polarizability of the sample, we therefore substantially cool the molecular gas using techniques developed previously and discussed in detail elsewhere[15]: the warm molecules are injected into a cryogenic buffer gas cell thermally anchored to a closed-cycle pulse-tube refrigerator and cooled to a temperature of ~7 K. However, other sources of cold molecules could also be used. A natural choice would be a pulsed supersonic beam source (rotational temperature ~2 K), which is frequently used as a cold molecule beam source for Fourier transform microwave spectroscopy[16].

The experimental set-up, sketched in Fig. 3, has two walls of the cryogenic cell formed by mirrors that comprise a tunable plano-concave Fabry–Pérot microwave cavity. The cavity is used to excite and detect the molecules, with each of its transverse and longitudinal spatial modes supporting two (degenerate) modes of orthogonal polarization. These modes can be separately addressed via waveguides attached to the planar mirror and coupled to the cavity via apertures (denoted A and B in

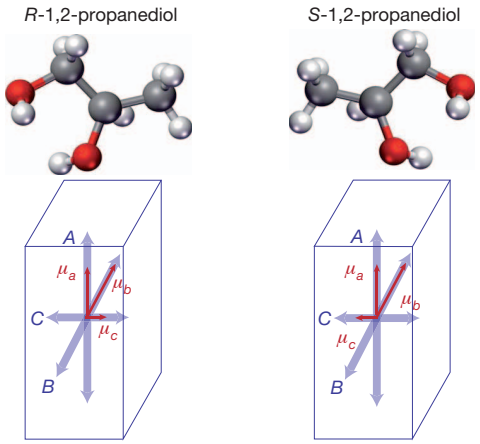

Figure 1 | The two enantiomers of chiral 1,2-propanediol. The Hamiltonian of a rigid chiral molecule in an external electric field is enantiomer-dependent. In any chiral molecule, opposite enantiomers have the same rotational constants A, B and C, and the same magnitude of dipole moment components $|\mu_a|$, $|\mu_b|$ and $|\mu_c|$, but the sign of the combined quantity $\mu_a\mu_b\mu_c$ is distinct for each enantiomer, independent of choice of axes. The displayed orientation of the molecules is for illustrative purposes.

[1]Department of Physics, Harvard University, Cambridge, Massachusetts 02138, USA. [2]Center for Free-Electron Laser Science, D-22607 Hamburg, Germany. [3]Max-Planck-Institut für Kernphysik, D-69117 Heidelberg, Germany.

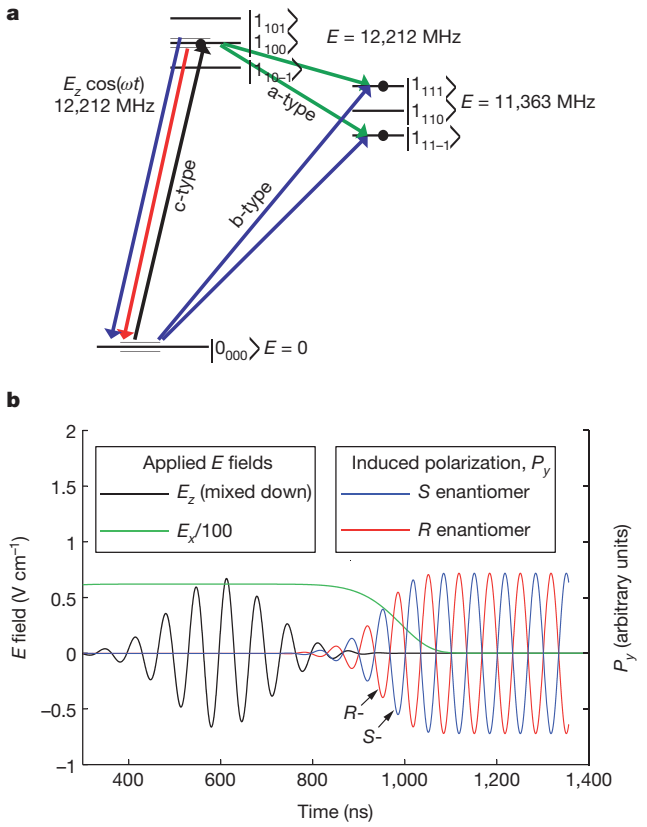

Figure 2 | 1,2-propanediol as a rigid rotor. **a**, The relevant rotational level structure of 1,2-propanediol. Each state is designated with $|J_{k_{-1}k_1 m}\rangle$. Molecules initially in the ground state are prepared in a superposition of $|0_{000}\rangle$ and $|1_{100}\rangle$ via a c-type microwave transition. A change in the electric field E_x mixes in components of $|1_{101}\rangle$ and $|1_{10-1}\rangle$ with complex phases proportional to μ_a. Allowed electric dipole radiation between these admixed states and the ground state produces an oscillating electric field in the laboratory $\hat{y}$ direction via a b-type transition. In the relevant limit of small E_z and E_x, this electric field E_y is proportional to $\mu_a\mu_b\mu_c$ and therefore changes sign with enantiomer. The applied field E_x of 65 V cm^{-1} induces a 500 kHz Stark splitting in the $|1_{10m}\rangle$ states that is not relevant to the dynamics due to the short (~200 ns) duration of the field. Admixing with the $|1_{01}\rangle$ state at 6,431 MHz (not shown) also contributes a small amount to the chiral signature. **b**, A simulation of 1,2-propanediol in applied electric fields E_z (microwave) and E_x. The frequency of E_z is 12,212 MHz, corresponding to the $|0_{00}\rangle \rightarrow |1_{10}\rangle$ c-type transition. In the figure, this field is mixed down to 15 MHz for clarity. Also shown is the simulated molecular polarization P_y for each enantiomer, induced by the change in the time-varying electric field E_x. P_y oscillates at the same 12,212 MHz frequency as E_z, and is also shown mixed-down to 15 MHz for visibility. The enantiomer-dependent phase of P_y is evident. To within experimental uncertainty, the sequence of applied fields shown here corresponds to the fields used to produce the enantiomer-dependent signals shown in Fig. 4.

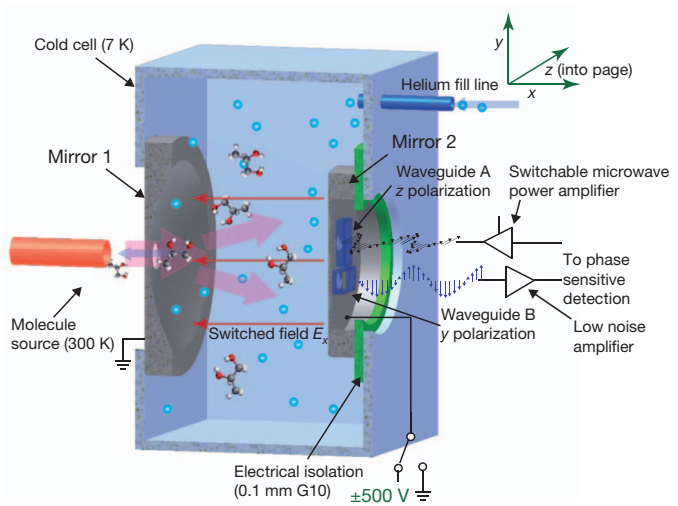

Figure 3 | A cryogenic buffer gas Fourier transform microwave spectrometer that provides enantiomer-specific detection. Molecules are introduced into a cryogenic cell from a room-temperature tube held close to an aperture in mirror 1. Microwave radiation is introduced using waveguides via coupling apertures in mirror 2. This mirror can be rapidly switched between ±500 V and ground, applying a time-varying electric field in the $\hat{x}$ direction; it is insulated from the cell by G10 fibreglass. The molecules are polarized initially in the $\hat{z}$ direction via a linearly polarized microwave pulse coupled from waveguide A. The resulting enantiomer-specific radiation is coupled out of the cavity via waveguide B, which is oriented to detect $\hat{y}$-polarized microwaves.

Fig. 3). A time-varying electric field E_x parallel to the cavity axis can be applied by rapidly changing the voltage of the planar mirror ($V_{\mathrm{mirror}} = \pm 500$ V, $E_x = \pm 65$ V cm^{-1}); this voltage is controlled with high-voltage switches with a switching time of ~100 ns.

In the experiments, molecules enter the cell continuously from a warm (300 K) feed tube and immediately start to cool through collisions with the cold helium buffer gas. By the time they diffuse into the central region of the cell, they have reached a rotational temperature of ~7 K. The cold molecules remain in the gas phase as they diffuse through the cell for several milliseconds, until they arrive at a cold cell wall and freeze there. Our detected signal comes only from the cold gas-phase molecules. The experimental sequence of applied electric fields begins with the application of E_x (see Fig. 3). The cavity is then driven with a strong, linearly polarized microwave field $E_z(t) = \hat{z}E_{\mathrm{mw}}\cos(\omega t)$. Here t is time, $\hat{z}$ is the unit vector along z, and E_{mw} is the field strength of the applied microwave field in the z direction. The excitation frequency ω is tuned to the $|0_{00}\rangle \rightarrow |1_{10}\rangle$ rotational transition of the ground-state conformer of 1,2-propandiol at 12,212 MHz. (We use the $|J_{k_{-1}k_1}\rangle$ nomenclature of ref. 8, where k_{-1} and k_1 indicate the quantum numbers of the limiting prolate and oblate symmetric top respectively; when m is specified, we use $|J_{k_{-1}k_1 m}\rangle$).

The maximum magnitude of E_z and the pulse length τ are adjusted to make $|\Omega|\tau \lesssim \pi/2$ for all molecules, where Ω is the Rabi frequency. This $\hat{z}$-polarized microwave pulse induces an oscillating electric dipole polarization, P_z, in the molecular ensemble. The electric field E_x is set to zero 200 ns after the end of the microwave pulse; E_x is switched over about 100 ns—rapidly compared to the molecular dephasing but slowly compared to ω. The change in E_x induces a sizable fraction of the oscillating molecular dipole to radiate at the same frequency ω with $\hat{y}$ polarization. Under our experimental conditions, the chirality-dependent polarization P_y has about 10% of the amplitude of P_z. The induced field E_y, which has an enantiomer-dependent phase, is amplified and recorded. The molecules continue to radiate in this manner until they rethermalize rotationally via collisions with helium atoms, typically after about 5 μs. This completes the experimental cycle, which can be started again by turning E_x back on. As in conventional Fourier transform microwave spectroscopy, molecules in distinct parts of the cavity radiate constructively into the original cavity mode used to polarize the sample. This important advantage is retained here because modes with orthogonal polarizations share an identical spatial structure.

Figure 4 shows averaged signals for the S and R enantiomers of 1,2-propanediol, and for a racemic mixture. Each signal represents the difference between a time trace taken with $E_x = +65$ V cm^{-1} and a trace taken with $E_x = -65$ V cm^{-1}. As predicted, the S and R enantiomers show a clear 180° phase shift. The opposite enantiomers and a racemic mixture are resolved with exceptionally high confidence. Our Hamiltonian integration calculations (shown in Fig. 2) are in excellent agreement with experimental data.

We note that the common spectroscopic methods of circular dichroism and vibrational circular dichroism can resolve spectral signatures sufficiently to deconvolve a chiral mixture that is comparatively simple[17],

whereas our method has the ability to identify an enantiomer amid a complex mixture of many other (possibly chiral) components. Although the chiral signature could be misread as for a different molecule, this would only occur in the very unlikely case of a second molecule having a rotational transition within the frequency range of the observed free-induction decay (in this case 12,212.14 ± 0.02 MHz). We expect that straightforward improvements to the electronics will allow us to resolve enantiomers present in concentrations as low as one part per thousand in a complex mixture, and that combining our method with broadband chirped-pulse spectroscopy techniques[18] will enable rapid and simultaneous species-specific and enantiomer-specific identification of many chiral components in a complex mixture.

Any coherent method of enantiomer-specific analysis can in principle be converted into a method of enantiomer purification[13,19–21], which could be realized here by adding a third, phase-controlled field pulse E_y; appropriate choice of the phase of E_z, E_x and E_y would transfer molecules of only one enantiomer to an excited state that could then be selectively addressed by additional fields.

We have applied our method to a single molecular species, but our simulations have identified applicable microwave transitions in a wide range of molecules. The only essential requirement is that the target molecule has at least one conformer with non-zero dipole moment components μ_a, μ_b and μ_c. Larger molecules, including most chiral molecules, typically exhibit several stable conformers and it is overwhelmingly likely that at least one of them meets this criterion. Our simulations of the enantiomer-dependent signals for molecules as diverse as carvone, nicotine and alanine predict a strong signal in every case, and we therefore expect that the upper size limit of molecules amenable to this technique is set by the limitations of gas-phase microwave spectroscopy (which has been used to characterize neurotransmitters, amino acids and drugs[22–24]). Furthermore, the absolute configuration of previously uncharacterized molecules could be resolved by using the technique presented here. The relevant molecular constants of 1,2-propanediol and the molecules listed above were calculated from the microwave spectra of cold molecular samples; such spectra are also measurable in our apparatus.

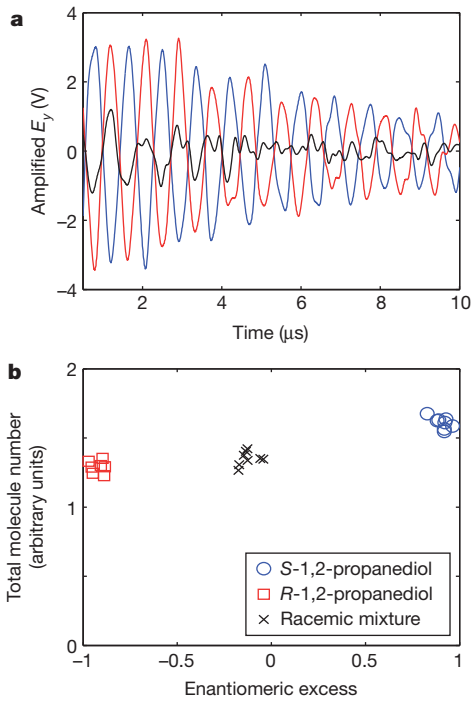

Figure 4 | Enantiomer-dependent microwave radiation. a, The enantiomer-dependent free-induction decay traces for *S*-1,2-propanediol (blue trace), *R*-1,2-propanediol (red) and racemic 1,2-propanediol (black). As predicted, opposite enantiomers show a 180° phase difference. **b**, Repeated measurements of enantiomeric excess (horizontal axis) and of total molecule number (vertical axis) for *S*-, *R*- and racemic 1,2-propanediol. Each data point represents about 20 s of experimental time, and 1 mg of sample. Enantiomers are clearly resolved.

METHODS SUMMARY

Enantiopure *R*-1,2-propanediol and *S*-1,2-propanediol (Sigma Aldrich) were used. The free-induction decay signals were recorded using standard Fourier transform microwave spectroscopy techniques[16], with a typical polarization pulse length of 200 ns. The signal was amplified, mixed down to an intermediate frequency of 20.2 MHz, further amplified, and digitized by a fast signal averager (Agilent U1084). Each data point in Fig. 4b represents 140,000 averages, about 20 s of experimental time, and 1 mg of 1,2-propanediol. The apparatus used here could identify the absolute configuration of an unknown enantiomer with 99% accuracy in less than 50 ms.

Full Methods and any associated references are available in the online version of the paper.

Received 14 December 2012; accepted 22 March 2013.

1. Busch, K. W. & Busch, M. A. (eds) *Chiral Analysis* (Elsevier, 2006).
2. Fischer, P. & Hache, F. Nonlinear optical spectroscopy of chiral molecules. *Chirality* **17,** 421–437 (2005).
3. Fischer, P., Wiersma, D. S., Righini, R., Champagne, B. & Buckingham, A. D. Three-wave mixing in chiral liquids. *Phys. Rev. Lett.* **85,** 4253–4256 (2000).
4. Li, Y. & Bruder, C. Dynamic method to distinguish between left- and right-handed chiral molecules. *Phys. Rev. A* **77,** 015403 (2008).
5. Rhee, H., Choi, J.-H. & Cho, M. Infrared optical activity: electric field approaches in time domain. *Acc. Chem. Res.* **43,** 1527–1536 (2010).
6. Hiramatsu, K. *et al.* Observation of Raman optical activity by heterodyne-detected polarization-resolved coherent anti-Stokes Raman scattering. *Phys. Rev. Lett.* **109,** 083901 (2012).
7. Hirota, E. Triple resonance for a three-level system of a chiral molecule. *Proc. Jpn Acad. B* **88,** 120–128 (2012).
8. Townes, C. & Schawlow, A. *Microwave Spectroscopy* (Dover Publications, 1975).
9. Darquié, B. *et al.* Progress toward the first observation of parity violation in chiral molecules by high-resolution laser spectroscopy. *Chirality* **22,** 870–884 (2010).
10. Quack, M. How important is parity violation for molecular and biomolecular chirality? *Angew. Chem. Int. Edn* **41,** 4618–4630 (2002).
11. Schnell, M. & Küpper, J. Tailored molecular samples for precision spectroscopy experiments. *Faraday Discuss.* **150,** 33–49 (2011).
12. Quack, M., Stohner, J. & Willeke, M. High-resolution spectroscopic studies and theory of parity violation in chiral molecules. *Annu. Rev. Phys. Chem.* **59,** 741–769 (2008).
13. Jacob, A. & Hornberger, K. Effect of molecular rotation on enantioseparation. *J. Chem. Phys.* **137,** 044313 (2012).
14. Lovas, F. J. *et al.* Microwave spectrum of 1,2-propanediol. *J. Mol. Spectrosc.* **257,** 82–93 (2009).
15. Patterson, D. & Doyle, J. M. Cooling molecules in a cell for FTMW spectroscopy. *Mol. Phys.* **110,** 1757–1766 (2012).
16. Balle, T. J. & Flygare, W. H. Fabry-Perot cavity pulsed Fourier transform microwave spectrometer with a pulsed nozzle particle source. *Rev. Sci. Instrum.* **52,** 33–45 (1981).
17. Guo, C. *et al.* Determination of enantiomeric excess in samples of chiral molecules using Fourier transform vibrational circular dichroism spectroscopy: simulation of real-time reaction monitoring. *Anal. Chem.* **76,** 6956–6966 (2004).
18. Brown, G. G. *et al.* A broadband Fourier transform microwave spectrometer based on chirped pulse excitation. *Rev. Sci. Instrum.* **79,** 053103 (2008).
19. Král, P., Thanopulos, I., Shapiro, M. & Cohen, D. Two-step enantio-selective optical switch. *Phys. Rev. Lett.* **90,** 033001 (2003).
20. Thanopulos, I., Král, P. & Shapiro, M. Theory of a two-step enantiomeric purification of racemic mixtures by optical means: the D_2S_2 molecule. *J. Chem. Phys.* **119,** 5105–5116 (2003).
21. Gerbasi, D., Brumer, P., Thanopulos, I., Král, P. & Shapiro, M. Theory of the two step enantiomeric purification of 1,3 dimethylallene. *J. Chem. Phys.* **120,** 11557–11563 (2004).
22. Pate, B. H&. De Lucia, F. C. (eds) Special issue: Broadband molecular rotational spectroscopy. *J. Mol. Spectrosc.* **280,** 1–2 (2012).
23. Mata, S., Peña, I., Cabezas, C., López, J. & Alonso, J. A broadband Fourier transform microwave spectrometer with laser ablation source: the rotational spectrum of nicotinic acid. *J. Mol. Spectrosc.* **280,** 91–96 (2012).
24. Grabow, J.-U. *et al.* Rapid probe of the nicotine spectra by high-resolution rotational spectroscopy. *Phys. Chem. Chem. Phys.* **13,** 21063–21069 (2011).

Acknowledgements We thank D. DeMille, A. Vutha and C. Connolly for discussions, and D. DeMille and C. Connolly for contributions to the final manuscript.

Author Contributions D.P. had the idea for this work, built the apparatus and produced the theoretical simulations. J.M.D. and D.P. developed experimental approaches and designed the apparatus. D.P. and M.S. performed the measurements. All authors wrote the manuscript.

Author Information Reprints and permissions information is available at www.nature.com/reprints. The authors declare competing financial interests; details are available in the online version of the paper. Readers are welcome to comment on the online version of the paper. Correspondence and requests for materials should be addressed to D.P. (dave@cua.harvard.edu).

METHODS

Numerical simulations. For a given sequence of applied fields, the simulation proceeds as follows: the matrix representations of the field-free Hamiltonian H_0 and the three Cartesian components of the dipole moment operator $\hat{\mu}_j$ ($j = x,y,z$) are calculated following ref. 8. The off-diagonal elements in these matrices are enantiomer dependent. The matrices are calculated in the oblate symmetric top basis with an arbitrary cut-off of rotational quantum number $J \leq J_{\max}$. $J_{\max} = 2$ for the simulation results shown in Fig. 2.

Molecules are assumed to start in an eigenstate of $\hat{H}_0$, $\psi(t=0) = \psi_{Jk_{-1}k_1m}$. For each time step Δt the electric fields to be applied at time t are calculated, and the Hamiltonian $\hat{H}(t) = \hat{H}_0 - E_x(t)\mu_x - E_y(t)\mu_y - E_z(t)\mu_z$ for an asymmetric top subject to those fields is calculated. Ψ is then evolved, according to:

$$\psi(t+\Delta t) = e^{\frac{-i\hat{H}(t)\Delta t}{\hbar}}\psi(t)$$

The time step Δt is chosen to be significantly faster than any frequency in the simulation. The induced laboratory-frame polarizations $P_j = \langle \mu_j \rangle$ are then calculated. $P_y(t)$, which has an enantiomer-dependent phase for our choice of applied fields, is plotted in Fig. 2. To simulate a thermal ensemble, this procedure is repeated for all initial states Ψ_0 up to $J = J_{\max}$ and the resulting polarizations, weighted by the Boltzmann factor $e^{-\varepsilon/k_BT}$ for each initial state, are summed to give the experimentally observable ensemble polarization. The validity of the simulations was checked by comparing predicted levels, line strengths and Stark shifts with the PGOPHER simulation package[25]. All simulations were written and performed in MATLAB.

Experimental details. Enantiopure *R*-1,2-propanediol and *S*-1,2-propanediol (Sigma Aldrich) were used. In the experiments, a flow rate of 1.5×10^{18} helium atoms s^{-1} into the cell provides an estimated in-cell helium density of 10^{14} atoms cm^{-3}. Approximately 5×10^{17} 1,2-propanediol molecules s^{-1} are sprayed towards the cell aperture; we estimate the 1,2-propanediol density within the cell to be about 10^{12} molecules cm^{-3}. The experimental repetition rate of 7 kHz is set (and limited by) the maximum switching frequency of our high-voltage switches. Without this limitation, or when E_x is set to zero, the rate is limited only by the molecular rethermalization rate of 200 kHz. The applied electric field E_x is $\pm 65\ V\ cm^{-1}$ (± 500 V on mirror 2). This high voltage is switched via Behlke HTS 151 high-voltage MOSFET switches. The polarizing pulse is typically 200 ns in duration, and our maximum microwave field E_z is estimated to be $0.5\ V\ cm^{-1}$ from measurements of the Rabi frequency Ω. The cavity was run in the $TEM_{11,n=6}$ mode; the more natural choice of the TEM_{00} mode could not be used because it was highly damped by loss through the molecule input aperture.

Mirror 2 of the cavity was mounted on flexible bellows and could be moved axially by about 1 cm, tuning the cavity (see Fig. 3 for cavity details). This tuning was accomplished via three thermally isolating, flexible shafts connected via rotary feedthroughs to knobs outside the Dewar. The aluminium cavity has a measured finesse of 105, a length of 8.1 cm, and a radius of curvature on its spherical mirror of 22.5 cm. The input aperture for the molecules has a diameter of 1.1 cm, and the coupling apertures A and B have diameters of 0.8 cm. The waveguides connected via apertures A and B are WR-62, operating from 12 to 18 GHz. E_y is detected after waiting $\sim$2 μs for the cavity to ring down. The signal is amplified by a low-noise amplifier (Pasternack PE1524) connected immediately outside the vacuum chamber with no protection diodes or switches. The amplified signal is mixed down to an intermediate frequency of 20.2 MHz, further amplified, and digitized by a fast signal averager (Agilent U1084). Each data point in Fig. 2b represents 140,000 averages, about 20 s of experimental time, and 1 mg of 1,2-propanediol. Our signal to noise ratio is sufficient to identify the absolute configuration of an unknown enantiomer with 99% accuracy in less than 50 ms.

The chirality-dependent signal E_y is proportional to E_xE_z. In order to cancel some systematic offsets in the detected microwave field, we exploit the change of sign of E_y with E_x by subtracting traces taken with equal and opposite values of E_x. This systematic offset in E_y arises from crosstalk between what are nominally orthogonal cavity modes. Even with this cancellation, the racemic 1,2-propanediol sample produces a small but statistically significant non-zero signal. A plausible explanation for this is imperfect reversal of our electric field; distinct MOSFET switches, resistor networks and power supplies are used for the positive-going and negative-going applied fields, and small errors in the voltage or timing could result in artefacts similar to those observed.

25. Western, C. M. *PGOPHER, a Program for Simulating Rotational Structure* Version 7.1 (Univ. Bristol, 2010).